PIMD-2π, a new variable for measurement of glaucoma
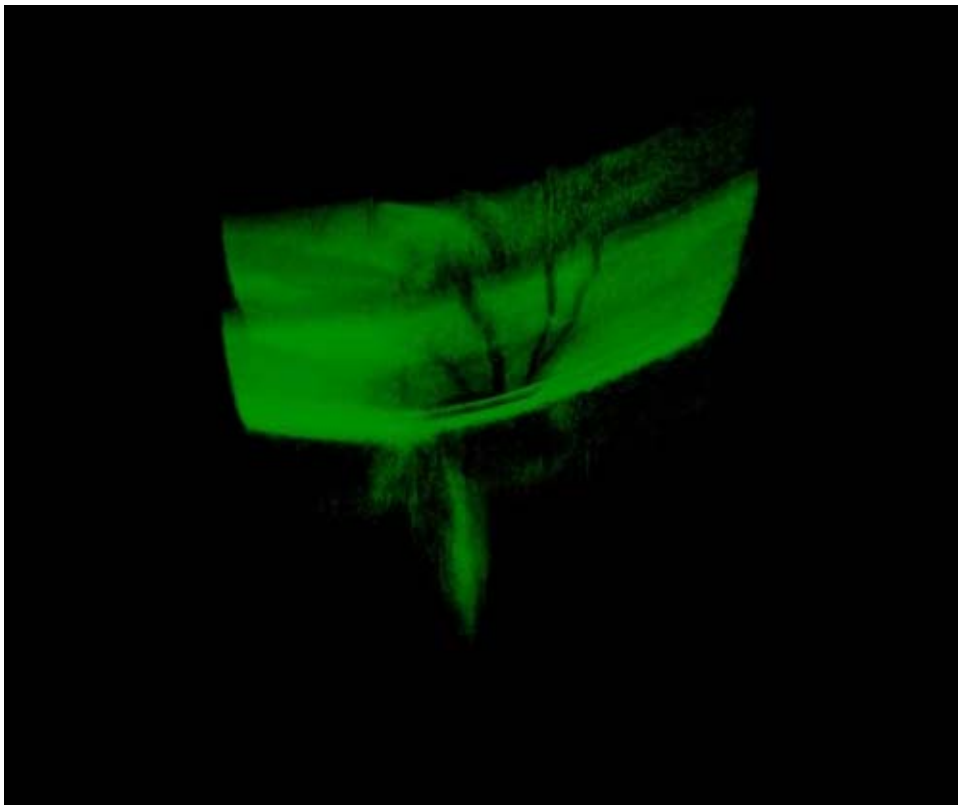
Sofia Eriksson

Handledare: Per Söderberg
Bihandledare: Camilla Sandberg Melin
2017-05-30

Titel: PIMD-2π, a new variable for measurement of glaucoma

Av: Sofia Eriksson

Innehåll

Populärvetenskaplig sammanfattning

Glaukom, eller grön starr som det också kallas, är världens näst vanligaste orsak till blindhet. Sjukdomen ger bortfall i synfältet på grund av att nervcellerna i synnervspapillen inne i ögat förstörs. Synnervspapillen är där näthinnans nervfibrer samlas ihop och tillsammans bildar synnerven.

Synfältsförlusten kommer ofta sent i sjukdomsförloppet, när många nervceller redan gått förlorade. Därför är det viktigt att upptäcka glaukom tidigt så att behandling kan ges och förhindra att symptomen förvärras. Flera av metoderna som används i kliniken idag är dock inte så känsliga som skulle önskas.

Med en relativt ny teknik som kallas optisk koherenstomografi (OCT) kan näthinnan och synnervspapillen avbildas snabbt och objektivt. Det är ungefär ljusets motsvarighet till ultraljud, och ger 3D-bilder av det man undersöker. Då kan nervcellslagrets tjocklek mätas, och därmed kan en förlust däri upptäckas.

I den här studien har en ny parameter för att mäta nervcellslagret i synnervspapillen med OCT testats på ögonfriska försökspersoner mellan 20 och 30 år. Parametern kallas PIMD-2π och är ett medelvärde av lagrets minsta tjocklek runt papillen, upplöst i 500 vinklar. Det undersöktes om mönstret av PIMD såg liknande ut mellan ögon inom individer, mellan individer, samt om PIMD-2π verkade bero av kön eller ögondominans. Ögondominans kan liknas med hänthet, fast för ögonen. I praktiken är ens dominanta öga det som används när man tittar i exempelvis ett teleskop.

Inga skillnader i PIMD-2π sågs mellan kvinnor och män, eller mellan dominanta och icke-dominanta ögon. Generellt var mönstren av PIMD runt papillen väldigt lika varandra. Nervcellslagret var tjockare i nedre och övre delen av papillen.

I framtiden är förhoppningen att kunna jämföra PIMD-2π-värden mellan flera olika åldersgrupper, och att göra metoden helt automatisk. Kanske kan den hjälpa till att diagnosticera och upptäcka försämring av glaukom med större känslighet än idag.

Abstract

Background: Through optical coherence tomography (OCT), the nerve fiber layer of the optic nerve head can be measured fast and non-invasively. This possibility for more objective follow-up of

glaucoma is proposed in a parameter termed Pigment epithelium central limit - Inner limit of the retina, Minimal Distance (PIMD). A semi-automatic algorithm for estimating PIMD around the circumference of the optic nerve head (PIMD-2π) has been developed and show promise to detect progress of glaucoma faster than conventional methods.

Purpose: To establish angular PIMD in healthy young adults and elucidate a possible dependence of PIMD-2π on gender and ocular dominance.

Method: Both eyes of 16 subjects, 8 of each gender and ocular dominance, were examined with a commercial SS-OCT device (DRI OCT Triton, Topcon, Japan). Three volumes of each optic nerve head of each eye were obtained.

Results: The 95 % confidence interval for difference in mean PIMD-2π between (1) women and men, (2) dominant and non-dominant eyes, and (3) dominant and non-dominant eyes in women and men respectively, all included zero.

Conclusions: There is a pattern in angular PIMD in the frontal plane. PIMD-2π does not seem to depend on gender or ocular dominance.

Background

Glaucoma is the second leading cause of blindness, and the leading cause of irreversible blindness, globally [1,2]. A recent study including the entire Danish population over the years 1996 through 2011 indicates a constant incidence of glaucoma, while the prevalence increases with an aging population. Prevalence numbers in 2011 ranged from 1,7 % for all ages, to 10 % for ages above 80 [3]. These numbers could be expected to be of similar size in Scandinavia or Sweden. No recent study of similar magnitude exists for the Swedish population.

The group of diseases that constitutes glaucoma is characterized by a slow loss of retinal ganglion cells, with changes in the optic disk and loss of visual field as a result [4,5]. It can broadly be classified as open-angle or angle-closure glaucoma and is often associated with increased ocular pressure. Early diagnosis is essential for halting disease progression.

Glaucoma diagnostics and follow-up
The methods used for diagnosis and follow-up of glaucoma today, however, do not enable diagnosis or determination of disease progression as early as desired. Symptoms of visual field loss may not arise until a relatively late stage. Visual field perimetry has high diagnostic accuracy, but is dependent on both patient participation and clinician interpretation. Further, a significant number of

glaucoma patients show optic disk defects before visual field loss occurs. Sommer et al. reported that nerve fiber loss was clinically visible 6 years before visual field loss first occurred, in 60 % of 1344 eyes with elevated intraocular pressure [6]. Other longitudinal studies have showed correlation between optic disk defects and development of visual field loss. Chauhan et al. found that patients with visual field loss were 3 times more likely to have had prior optic disk defects [7], while Medeiros et al. concluded that eyes with progressive optic disk damage had a 26 times higher risk of developing visual field defects [8]. Clearly, visual field testing must be combined with assessment of the optic disk appearance. This has traditionally been done with ophthalmoscopy, but therefore highly depends on the clinician's knowledge and performance [9].

More objective methods for glaucoma follow-up are sought. The most recent progress toward this is measuring nerve fiber layer thickness in the optic nerve head (ONH) using Optical Coherence Tomography (OCT) [10].

Anatomy of the optic nerve head
The ONH, or optic disk, is where the retinal ganglion cell axons leave the eye (Figure 1).
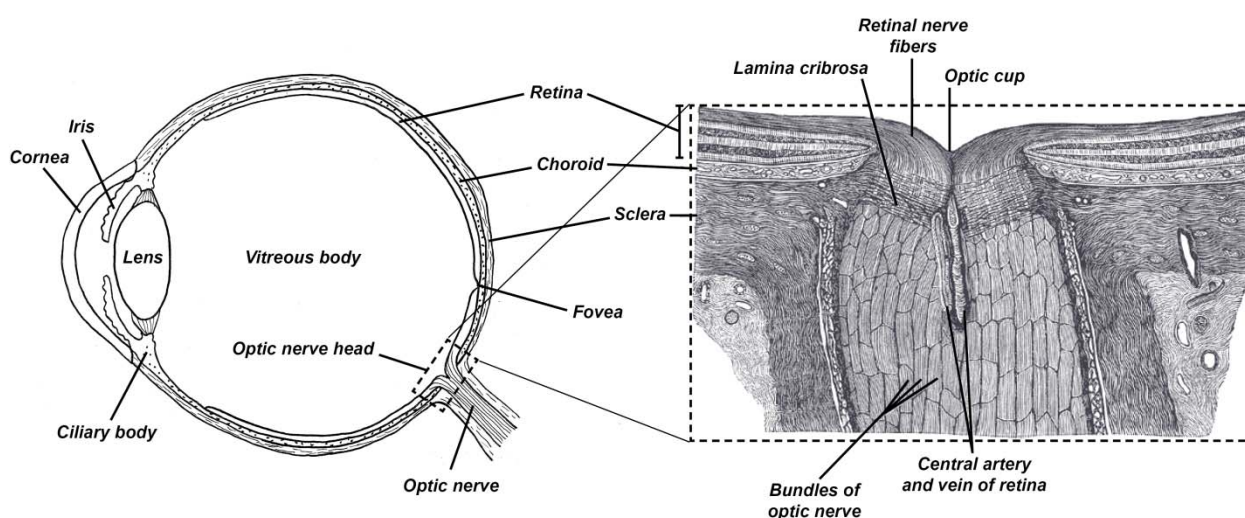
Figure 1. **Anatomy of the optic nerve head**. At the optic nerve head, the retinal ganglion cell axons leave the eye and form the optic nerve. (Illustration to the right reworked from Gray's Anatomy, 1918)

Together they form the optic nerve and carry information from the photoreceptors to the brain. The innermost layer of the retina - the nerve fiber layer, is adjacent to the vitreous body. The outermost layer - the pigment epithelium, is secured to the choroid. At the opening of the sclera, the nerve fibers dive towards the brain. [11,12] Here, in the neuroretinal rim around the edge of the ONH, more than 90 % of the volume are are ganglion cell fibers. The cup in the center of the ONH contains no nerve fibers. Glaucoma, with loss of axons, causes thinning of the neuroretinal rim and increased volume of the cup. The cup-to-disk ratio is a simplified measurement of this loss.

The size of the ONH, and the number of axons in it, varies among individuals [13]. Even without pathology a loss of axons occurs naturally with age [14]. Generally, the thickness of the nerve fiber layer is greater in the superior and inferior poles of the disk [15,16]. This creates a "double hump" pattern when visualizing the thickness as a function of ONH angle.

Optical Coherence Tomography

Through OCT, the retina and its layers can be imaged non-invasively with high resolution. OCT was first developed in the early nineties to facilitate examination of internal microstructures.[17] The technique is based on interferometry and coherence of optic radiation, and yields cross sections based on back-scattering from the examined tissue. This is achieved when radiation of low coherence length is sent through a semitransparent mirror, which splits the radiation beam into two; one part is guided to the test object (in this case the retina), and the other to a reference mirror (Figure 2).
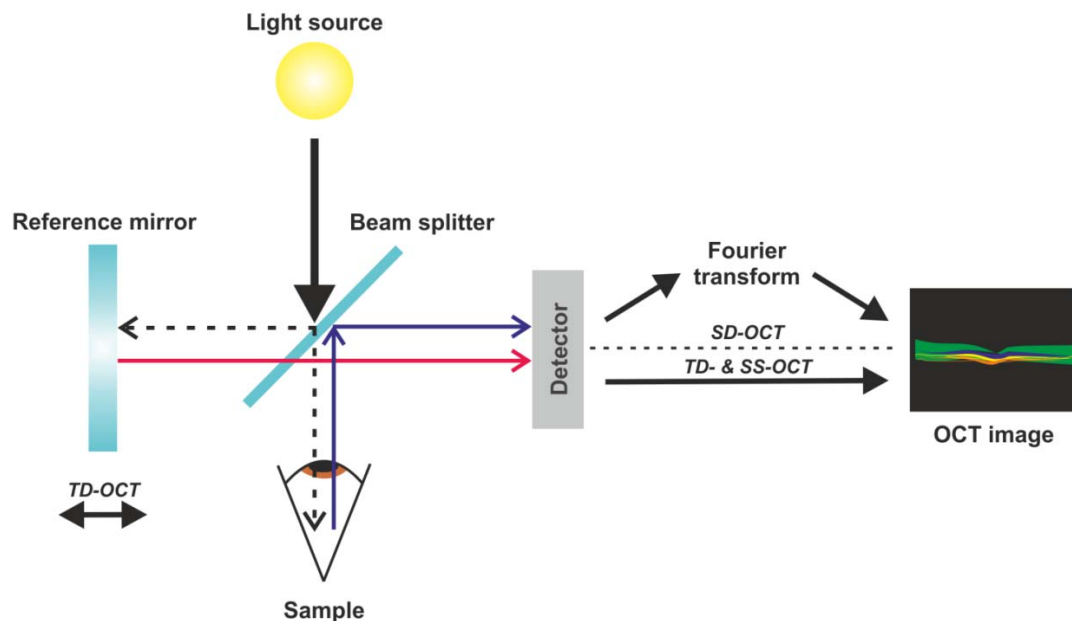
Figure 2. Principle of optical coherence tomography. The radiation from the light source is of low coherence in TD-OCT, of broadband low coherence in SD-OCT and of narrow bandwidth (swept through multiple wavelengths) in SS-OCT.

Back-scattered light from the retina interferes with the reflected light from the reference mirror. A signal is detected only if the waves of the two beams of light are within close phase of each other - i. e. if the scattered light from the retina reaches the detector in the same amount of time as the reference beam. The reference mirror is moved - thus changing the time of flight and scanning depth. Due to different reflectivity in the layers of the retina, scattering of different intensity is detected at various depths and combined into an A-scan. Several adjacent A-scans together constitute a B-scan - a 2D rendering.

The above described time domain OCT (TD-OCT) has during the last decades undergone further evolution. Spectral domain OCT (SD-OCT, also known as Fourier domain OCT) increases image resolution and drastically reduces the image capturing time by circumventing the need for mechanical movement of the reference mirror.[18] The shorter capturing time enables higher resolution images with fewer motion artefacts. SD-OCT uses a broadband radiation source, a fixed mirror and a spectrometer to detect backscattered light in the frequency domain. Light of different frequency travels with different speed in the tissue, due to dispersion. Therefore, back-scattering from different depths of the retina reaches the detector (a spectrometer) at the same time and interferes. The spectrometer outputs the interference pattern, which is then converted into an electric intensity signal. Through Fourier analysis the signal is transformed into spatial intensity information - an A-scan. The increased capturing speed of SD-OCT also allows adjacent B-scans to be combined into a 3D volume.

Swept-source OCT (SS-OCT)[19] is a further advancement in OCT imaging, and the technique used in the OCT-device in this study. As with SD-OCT, signals are detected in the frequency domain. In contrast, the radiation used is of narrow bandwidth, which with high speed is swept through a wide range of frequencies. The back-scattering from the retina at each frequency is detected with a photodetector. Each frequency corresponds to a defined depth in the retina. The signals from all the frequencies constitute the A-scan.

New methods for glaucoma follow-up

With OCT, the thickness of the nerve fiber layer (NFL) in the ONH can be measured. Since the axons of *all* nerve cells from the retina must pass through the narrow opening in the sclera, measuring the NFL here is advantageous in relation to estimating the nerve fiber loss in glaucoma. This stands in comparison to measurement of the retinal nerve fiber layer (RNFL) "further out" - peripapillary, as is done with older scanning methods. This potential for more objective glaucoma follow-up has been recognized by several authors. However, it is not yet established which structure to measure, to render the best representation of the nerve fiber loss.

Povazay et al. proposed Minimum Circumpapillary Band (MCB) as a parameter for NFL thickness quantification with SD-OCT. MCB is defined as the shortest distance between the inner limiting membrane and Elsching's ring (which coincides with the retinal pigment epithelium), over the circumference of the ONH [20]. Compared to previous methods using TD-OCT, Povazay argued that MCB would be a better estimate of the NFL, which due to tilting of the optic disk is more accurately visualized in 3D. Chen et al. further studied this concept, but retermed it Minimal Distance Band (MDB), and found good correlation to clinical examination.[21] In a more recent

study, the MDB parameter combined with an automatic segmentation algorithm demonstrated a higher diagnostic ability than TD-OCT methods in multiple regions of the ONH [22].

Reis et al. has suggested that SD-OCT imaging can measure nerve fiber structure which size may be over- or underestimated through clinical examination only. They used a parameter termed Bruch's Membrane Opening - Minimum Rim Width (BMO-MRW), defined as the minimum distance between Bruch's membrane (the innermost layer of the choroid) and the internal limiting membrane [23,24]. In similarity with above described methods, this way of measuring takes the orientation of the axons in the ONH into account. A 2013 study indicated that BMO-MRW has a higher sensitivity in differentiating glaucoma from healthy eyes, compared to older NFL-scanning methods [25].

The minimum distance between the central limit of the pigment epithelium and the inner limit of the retina, averaged over 2π radians, is proposed as a new variable for measurement of glaucoma.[26] This distance is termed Pigment epithelium central limit - Inner limit of the retina, Minimal Distance (PIMD) (Figure 3).
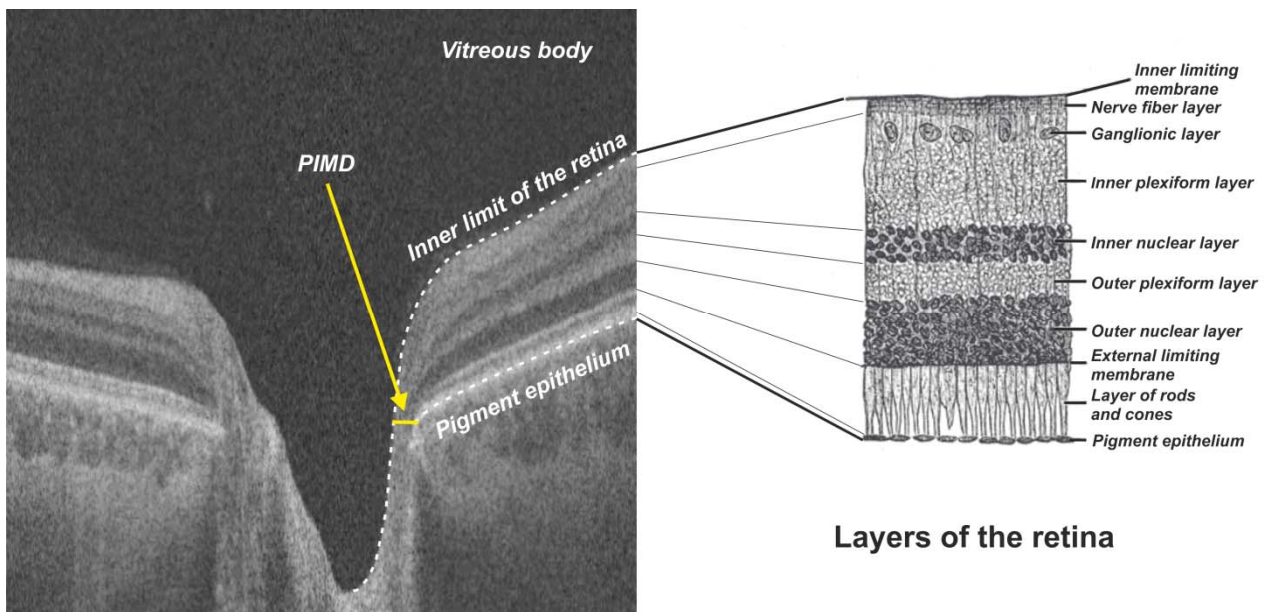
Figure 3. Definition of PIMD (Pigment epithelium central limit – Inner limit of the retina, Minimal Distance), as visualized in one OCT B-scan. The layers of the retina are marked as they appear in the OCT image. (Illustration to the right reworked from Gray's Anatomy, 1918)

A semi-automatic segmentation algorithm for estimation of PIMD over the circumference of the ONH, in the frontal plane (PIMD-2π) has been developed [27]. The ONH is captured in 3D cubes using SD-OCT. A recent study including 13 glaucoma patients indicated that PIMD-2π measurements can show glaucoma progression several years earlier than conventional methods [28]. Assuming a 10 per cent loss of PIMD in a segment, per year, a significant change in PIMD-2π in 18

months. This is to be compared with 3 years with Humphrey visual field perimetry, and 4-5 years measuring the neuroretinal rim using Heidelberg retinal tomography.

To be able to use methods such as those described above in clinical everyday practice, they need to be fast. Automatic algorithms built into the OCT device is a way of achieving that. Currently, algorithms have been designed for the Cirrus [29] and Spectralis [30] OCT devices.

Ocular dominance

Ocular dominance is comparable to handedness; ones dominant eye is the one from which visual input is preferred. In a practical sense - the eye used when looking through a telescope or microscope, for example. Around two-thirds of people are right-eye dominant [31,32].

There is no golden standard for determining ocular dominance. Several tests exist, most of which are subjective. Seijas et al. found poor correlation between different tests, and concluded that some individuals may lack a definitive ocular dominance [33].

The correlation between ocular dominance and the configuration of the nerve fiber layer in the optic disk is a scarcely studied subject. Several PubMed searches with different combinations all including '(Dominance, ocular)' yields only two relevant publications [34,35]. Comparisons between right and left eyes have been made, but without consideration to ocular dominance [36,37].

Purpose

The purpose of the present investigation was to establish angular PIMD in healthy young adults. Further, it was intended to elucidate a possible dependence of PIMD-2π on gender and ocular dominance.

The questions sought to answer were: Is there a difference in PIMD-2π between women and men? Is there a difference in PIMD-2π between dominant and non-dominant eyes, among individuals, and among women and men (respectively)? Does PIMD-2π depend differently on ocular dominance between genders?

Method

Subjects

Volunteers participated in the study after written informed consent was obtained. Inclusion criteria are listed in Table 1.

Table 1. Inclusion criteria

Variables	Criteria
Age (years)	20<, < 30
Refractive error (D)	> -5, < 5
No previously diagnosed eye disease	
Lack of condition that makes OCT examination impossible	

All inclusion criteria were self-reported. It was planned to exclude any subject presenting with a condition that made OCT imaging impossible during the course of the study.

Ethical approval was not required since the present is a student project not intended for publication.

Procedure

Eye dominance was determined with a variation of the Miles test/"hole-in-hands-test" [38]. The test implies that the subject extends both arms forwardly, form a small hole with their hands, center an object in the center of the hole and close one eye at a time. The eye that yielded least movement of the object was considered dominant. Instruction for eye dominance testing was given in writing prior to examination, and the result was reported by the subject.

Examinations were performed at the ophthalmology clinic at Uppsala Akademiska sjukhuset. Subjects were anonymized through a coding system and no personal information was associated with the research data.

OCT imaging

At 20-30 minutes prior to OCT examination, the pupils of both eyes in each subject were dilated with Tropicamide, 5 mg/ml.

For OCT imaging, the light in the room was dimmed. Volumes of the ONH were obtained with a commercial OCT device (DRI OCT Triton, Topcon, Japan). The eye not being examined was occluded. All volumes were acquired with the same machine and by the same operator.

After appropriately positioning the subject for examination, the acquisition protocol *3D Macula cube, 7x7 mm* was chosen for subject identification of the fixation target (single green square). Then, the OCT protocol was switched to *3D Glaucoma disc, cube, 6x6 mm* and the device was focused.

Consecutive volumes were captured until three volumes of each eye with adequate quality were obtained. Volumes with artefacts due to eye movement involving the ONH, as judged by the OCT operator, were discarded. The subject removed and repositioned his/her head between images.

The scanning protocol captures data in 992 points along the sagittal axis. Therefore; the resolution of one A-scan is 992 points. 512 A-scans along the horizontal axis together form one B-scan, and 128 B-scans along the vertical axis form the 3D cube. Corresponding sizes in length are 2.8 x 6.0 x 6.0 mm, with one voxel[*] measuring 2.8 x 12 x 26 μm (Figure 4).
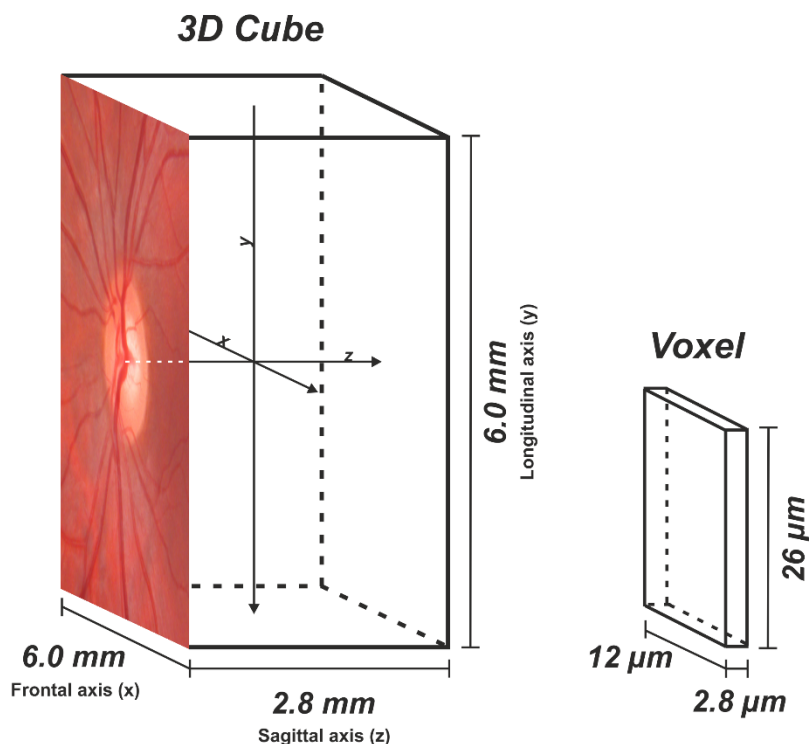
Figure 4. Schematic representation of the 3D cube and voxel size captured with the OCT device (DRI OCT Triton, Topcon, Japan).
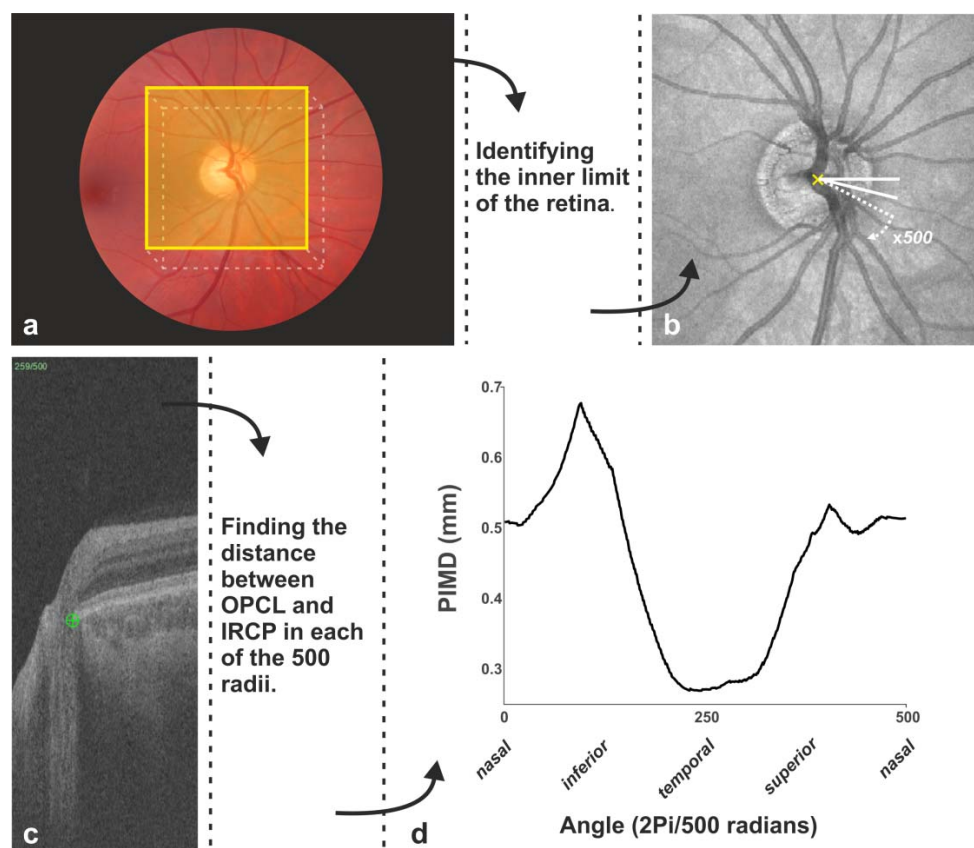
Estimation of PIMD-2π

For each scan of the ONH, the 3D volume of raw data was extracted from the Topcon DRI OCT Triton and exported to the numerical computing language MatLab. The inner limit of the retina was automatically identified and translated into points in a Cartesian coordinate system, rendering a 3D surface.

While viewing a frontal projection of the cube, the center of the ONH was manually approximated. The cube was then transformed into a polar coordinate system and divided into 500 equally spaced radial images centered on the ONH. The ONH Pigment epithelium Central Limit (OPCL) was manually selected by the same observer in a program specifically designed for this purpose. The observer first marked the position of the OPCL in a radial image where it was clearly discernible. All 500 radial images were then scrolled through consecutively, and the OPCL was marked when its location differed from the last marked position. For unmarked radial images, the location of the OPCL was estimated by linear interpolation from the two closest marked OPCLs. The manually

---

[*]A voxel is the 3D equivalent of pixel.

marked OPLCs outline the delineation of the ONH central limit of the pigment epithelium. The location of the delineation was then reintroduced into the Cartesian coordinate system.

Subsequently, an algorithm finds the closest corresponding point on the inner limit of the retina (Inner limit of the Retina Closest Point, IRCP) for each of the 500 locations of OPCL. The distance between two points of OPCL and IRCP represents PIMD (Figure 5). The mean value of PIMD for the 500 radii and, consequently, over the circumference of the ONH, is PIMD-2π.

Figure 5. Estimation of PIMD. (a) Fundus photo illustrating the frontal plane of an ONH volume scanned. (b) Manual approximation of the center of the ONH (yellow cross) in a frontal projection of the OCT captured volume. Based on this, the cube is divided into 500 equally spaced radial images. (c) Manual identification of OPCL (ONH Pigment epithelium Central Limit, green cross) in the 500 radii. (d) Graph showing PIMD as a function of angle in the captured 3D volume of the ONH.

Experimental design

In total, 16 subjects were examined. In each subject 3 volumes of the ONH of each eye were captured. Each volume consisted of 500 radii of PIMD distributed at equal angles over 2π radians. Of the subjects, 8 were women, and 8 were men. The median age of women was 23.98 years, and the median age of men was 25.25 years. Half the number of subjects of each gender was right eye dominant.

Each measurement of a woman was followed by a measurement of a man. Each measurement of a woman with right eye dominance was followed by a measurement of a man with right eye dominance. Further, dividing the subjects into subgroups of 4, the dominant eye was examined first

in the first and third subgroup, while the non-dominant eye was examined first in the second and fourth (Table 2).

Table 2. Measurement protocol.

Subject no.	Gender [♀=woman, ♂=man]	Eye dominance [R=right, L=left]	Eye measured first [D=dominant, N-D=non-dominant]
1	♀	R	D
2	♂	R	D
3	♀	L	D
4	♂	L	D
5	♀	R	N-D
6	♂	R	N-D
7	♀	L	N-D
8	♂	L	N-D
9	♀	R	D
10	♂	R	D
11	♀	L	D
12	♂	L	D
13	♀	R	N-D
14	♂	R	N-D
15	♀	L	N-D
16	♂	L	N-D

Statistical parameters

Considering the sample size and the contrasts aimed for, the confidence coefficient was set to 0.95.

Difference in mean PIMD-2π between women and men was estimated through calculation of the 95 % confidence interval for the difference between independent groups, with pooled variance. The same calculation was used for the difference in difference between dominant and non-dominant eye between women and men.

For comparisons of difference in PIMD-2π between dominant and non-dominant eyes, the 95 % confidence interval for difference between dependent groups was calculated.

If the confidence interval includes zero, there is no difference between the two groups compared.

Results

Reproducibility of angular PIMD among volumes within subject

To examine reproducibility among volumes within eye within subject, the second and the third volume was cross-correlated to the first volume. This was to find a possible phase shift among the

recordings of PIMD as a function of angle in the frontal plane. The original angular PIMD in the second and the third volume was then phase adjusted.

An examination of all the recordings of phase adjusted angular PIMDs in volumes within eye within subject revealed almost identical functions (Figure 6).
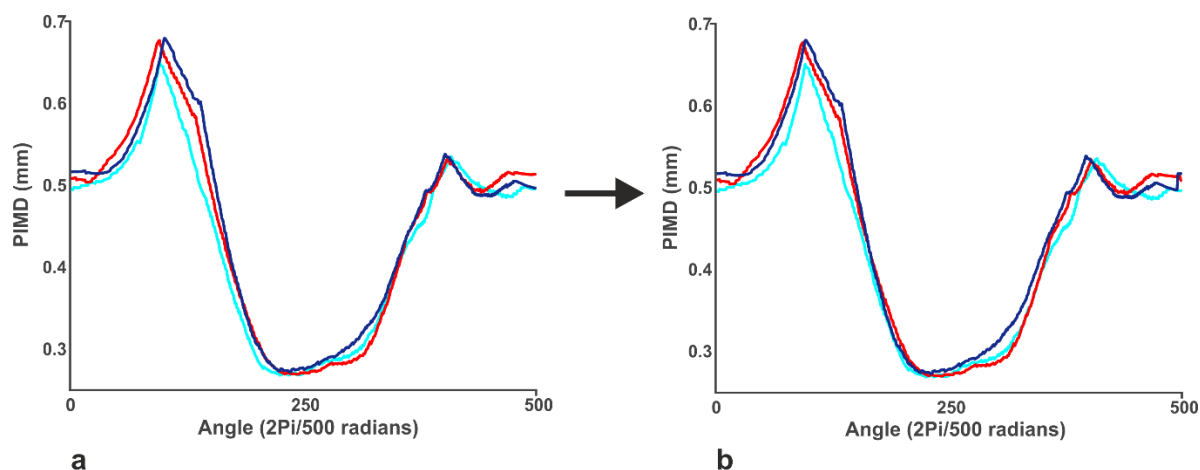
Figure 6. (a) Typical angular PIMD from three volumes of the optic nerve head in one eye from one subject. (b) Phase adjusted volumes.

Distribution of angular dependence of PIMD among subjects

To examine the angular PIMD between sides within subject, and among subjects, the phase adjusted angular PIMD for volumes within side within subject were averaged for each angle in the frontal plane. The resulting angular PIMDs reveled similar appearance both between eyes within subject and among subjects (**Error! Reference source not found.**).
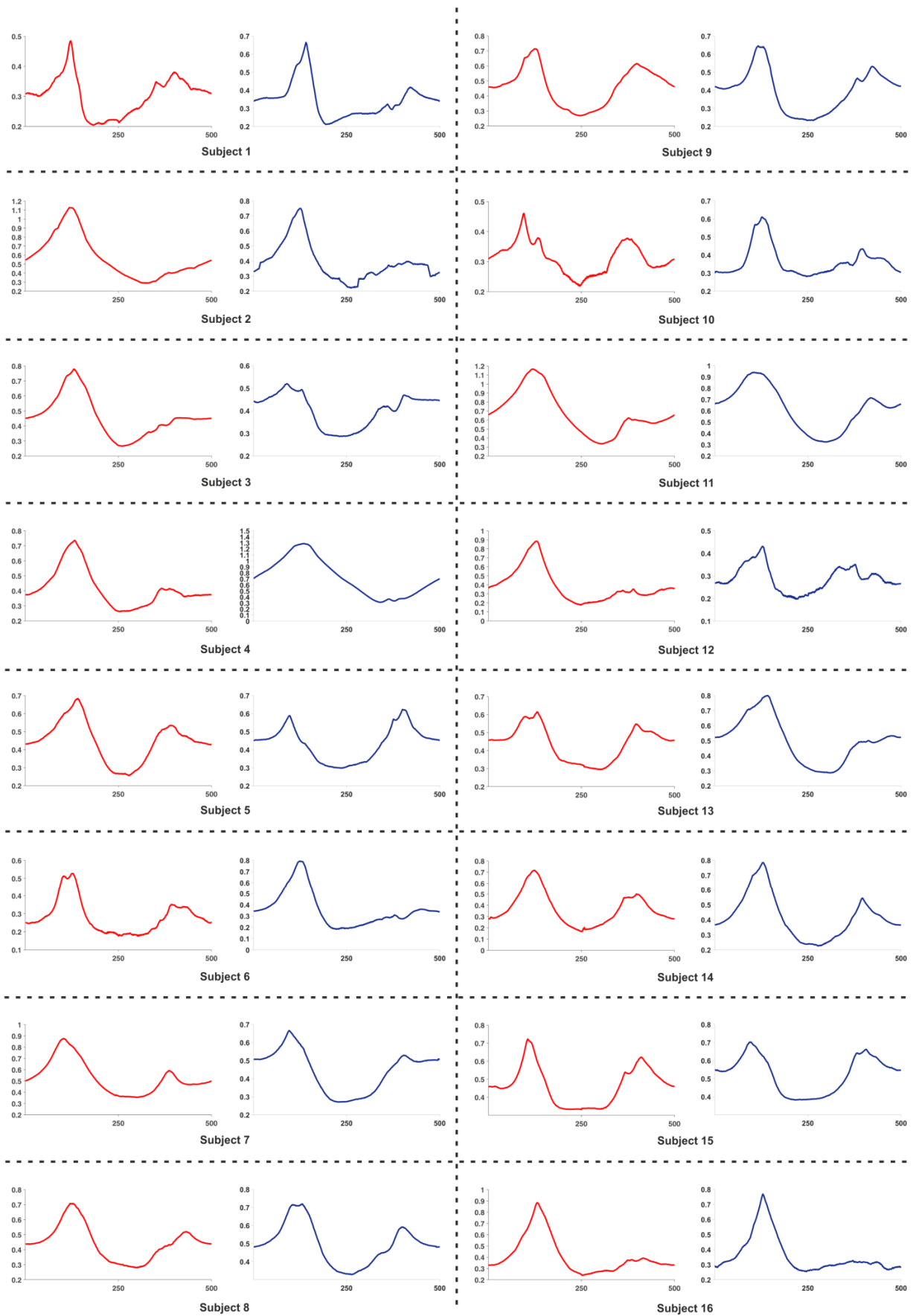
Figure 7. Angular PIMDs for phase adjusted volumes, averaged for each eye of each subject. Red curves represent left eyes, blue curves represent right eyes. The x-axes show angle (2π/500 radians), the y-axes show PIMD (mm).

Difference between women and men

The estimated 95 % confidence interval for the mean PIMD-2π was 470 ± 80 µm (d.f = 7) for women, and 410 ± 70 µm (d.f. = 7) for men. The 95 % confidence interval for the mean difference of PIMD-2π between women and men was 50 ± 100 µm (d.f. = 14) (Table 3).

Table 3. Dependence of estimated PIMD-2π on gender.

Confidence interval quantity	Estimated 95 % confidence interval for mean (PIMD-2π) (µm)	Degrees of freedom
Women	470 ± 80	7
Men	410 ± 70	7
Women – Men	**50 ± 100**	**14**

Difference between dominant and non-dominant eyes

The estimated 95 % confidence interval for the mean PIMD-2π was 440 ± 40 µm (d.f = 15) for dominant eyes, and 440 ± 70 µm (d.f. = 15) for non-dominant eyes. The 95 % confidence interval for the mean difference of PIMD-2π between dominant and non-dominant eyes was 0 ± 60 µm (d.f. = 15) (Table 4).

Table 4. Dependence of estimated PIMD-2π on gender and ocular dominance.

Confidence interval quantity	Estimated 95 % confidence interval for mean (PIMD-2π) (µm)	Degrees of freedom
Dominant eyes	440 ± 40	15
Non-dominant eyes	440 ± 70	15
Dominant – Non-dominant eyes	**0 ± 60**	**15**
Women, dominant eyes	480 ± 80	7
Women, non-dominant eyes	460 ± 80	7
Women: Dominant – Non-dominant eyes	**20 ± 50**	**7**
Men, dominant eyes	400 ± 20	7
Men, non-dominant eyes	430 ± 130	7
Men: Dominant – Non-dominant eyes	**-30 ± 120**	**7**
Gender difference: Dominant – Non-dominant eyes	**50 ± 130**	**9**

Difference between dominant and non-dominant eye in women and men, respectively

The estimated 95 % confidence interval for the mean PIMD-2π was 480 ± 80 µm (d.f = 7) and 460 ± 80 µm (d.f. = 7) for dominant and non-dominant eyes of **women**, respectively. The 95 % confidence interval for the mean difference of PIMD-2π between dominant and non-dominant eyes of **women** was 20 ± 50 µm (d.f. = 7) (Table 4).

The estimated 95 % confidence interval for the mean PIMD-2π was 400 ± 20 µm (d.f = 7) and 430 ± 130 µm (d.f. = 7) for dominant and non-dominant eyes of **men**, respectively. The 95 % confidence interval for the mean difference of PIMD-2π between dominant and non-dominant eyes of **men** was -30 ± 130 µm (d.f. = 7) (Table 4).

Difference in difference between dominant and non-dominant eye between women and men

The 95 % confidence interval for the mean difference in difference of PIMD-2π between dominant and non-dominant eyes between women and men was 50 ± 130 µm (d.f. = 9) (Table 4).

Analysis of variance

In order to exclude any systematic difference due to gender, ocular dominance or side the PIMD-2π measurements were first analyzed assuming a complete model. No systematic differences were found. Considering the results of the complete model analysis, the PIMD measurements were analyzed with a simplified model aiming to evaluate the sources of variation in the PIMD-2π estimates. In this model, each PIMD-2π measurement (x_{ijk}) is the sum of mean PIMD-2π (μ), a term for the random variation among subjects (A_i), sides ($B_{j(i)}$), and volumes ($\varepsilon_{k(ij)}$) (Eq. 1).

$$x_{ijk} = \mu + A_i + B_{j(i)} + \varepsilon_{k(ij)}$$ Eq. 1

It was found that the variation among subjects and sides was of the same order. The variation among volumes was of one magnitude lower (Table 5).

Table 5. Sources of variation in PIMD-2π estimations.

Source of variation	Variance (μm)^2	Degrees of freedom
Subjects	5310	
Sides	5480	
Volumes	610	64

Average PIMD-2π was estimated to 440 µm. The standard deviation for differences of the average of n volumes within the same eye, within the same subject, between two occasions, σ_{x_d} (µm) is given by Eq. 2. According to previous studies, the variance among occasions is negligible.

$$\sigma_{x_d} = \sqrt{2 \cdot \frac{\sigma_{Volumes}^2}{n}}$$ Eq. 2

Insertion of the variance for volumes in Table 5 into Eq. 2 yields a standard deviation for variance for difference between two occasions of 20 μm. Considering detection of a 10 % change per year of 440 μm (corresponding to a total loss in 10 years), the variation coefficient for detecting such a change is 45 %. If the number of volumes averaged per occasion is 10, the variation coefficient for detecting a 10 % change is approximately 25 %.

Discussion

The purpose of the present investigation was to establish angular PIMD in healthy young adults. Further, it was intended to elucidate a possible dependence of PIMD-2π on gender and ocular dominance. After plotting the three volumes' mean angular PIMD for the right and left eye, respectively, in each subject – a clear pattern could be observed. In addition, PIMD-2π does not seem to depend on gender or ocular dominance.

Results

Generally, no significant change was observed when phase adjusting the volumes within eyes. This implies that the subject positioned his-/herself similarly between each OCT image. The similar appearance of the three volumes also implies that the delineation process was performed in the same way for all volumes. Volumes delineated by two different persons might not look as similar.

Looking at Figure 7, it is worth noting that the scales of the y-axes in the graphs differ among each other. Since only the patterns of angular PIMD, and not the absolute values, are of interest - the scale of the y-axis does not impact the interpretation of the curves. It does however point to the large variation among individuals; with, for example, the highest measured PIMD in one subject being nearly three times the value of the highest in another. The PIMD pattern looks very similar between eyes of the same subject. So does the scales of the y-axes, except for subject 4 and 12. The reason for this could be natural, although odd, or perhaps because of blood vessel artefacts affecting the algorithms ability to recognize the inner limit of the retina. Or possibly, the blood vessels themselves give rise to a difference. Jee et al. found that interocular blood vessel location can influence the symmetry between the right and left RNFL thickness, more so than differences in refractive error between the eyes [36]. Similarly, Hwang et al. concluded that RNFL asymmetry existed, but did not depend on anisometropia [37]. Note that neither one of the above mentioned studies measured the nerve fiber layer in the ONH. Interocular symmetry has not been investigated with the BMO-MRW or MDB parameters.

Nearly all curves display a peak PIMD value around radii 175. That is - a thicker nerve fiber layer in the inferior pole of the ONH. This has been seen both histologically [15], and in investigations with the BMO-MRW [24] and MDB [21] parameters.

The lack of difference in mean PIMD-2π between women and men was also expected, as it complies with previous literature [16,39]. Men might have a slightly larger ONH [13], but since the number of nerve fibers doesn't differ between genders [14] it should not affect the thickness of the nerve fiber layer.

As for PIMD's dependence of ocular dominance, very few similar studies exist. Samarawickrama et al. examined the eyes of 6- and 12-year old children with TD-OCT, and found no clear structural differences in the RNFL between dominant and non-dominant eyes [34]. Choi et al. studied the eyes of adult Korean males with SD-OCT, and saw thicker inferior RNFL compared to superior RNFL in dominant eyes only [35]. One could speculate that the reason why dominant ONHs might have thicker nerve fiber layer is because they are "used" more and therefore have a higher number of nerve cells. Maybe, the present investigation had a too small size to discover a difference. More studies are needed to clarify the correlation between nerve fiber layer thickness and ocular dominance.

Method

The sample in this study had several limitations. It was of small size, and not very closely defined. Drawing conclusions from comparisons between groups of only 8 people is not optimal. The confidence interval for difference in PIMD-2π between women and men had a ß-error of 0.82, which implies a high risk of accepting that no difference exists in the sample population even if there is one. The sample size was accepted considering that the present study is a pilot study and a student project with a limited time frame.

Self-reported variables in the inclusion criteria involved a risk of including subjects that did in fact not meet the criteria. However, that risk was most likely small, considering that the subjects were young (and therefore healthy) and had little personal gain from participating in the study. Assessing visual acuity and refractive error before OCT examination would have been desirable, but was abstained from due to time constraint. The ONH in eyes with high myopia has been found to have a higher degree of tilt [40,41], which could have an impact on OCT measurements of the nerve fiber layer. Astigmatism also correlates to the tilt of the ONH [42], but was not taken into consideration in the present study.

A problem with self-reporting also applies to the determination of ocular dominance. The subjects received instructions for testing dominance in writing prior to the examinations. At the time of

examination, the subjects orally confirmed their results. Obviously there's an uncertainty here - did the subjects all perform the test correctly and in the same way as one another? In addition, ocular dominance is difficult to test and no golden standard exists. An individual's dominant eye may differ depending on viewing distance, or perhaps not be clearly defined at all [33]. The variation of the Miles test that was used in this study however performed somewhat better than others in a comparison of several tests [33].

The operator of the OCT device was inexperienced and probably improved in skill during the course of the study - a factor that may have had an effect on the quality of the examinations. In order to minimize the effect of this, the measurement protocol was set up as to distribute gender and eye dominance evenly in the examination order. The same operator determined which OCT images were of adequate quality. Any volumes that later during the PIMD estimation process were found to have unacceptable movement artefacts were to be discarded. However, no volume differed enough from the other two within the same eye to have to go through rejection.

No ethical approval was obtained for the project. Nevertheless, the examinations were conducted with an ethical perspective in mind. Subjects were anonymized in a coding system and no personal information was associated with the research data. The eye drops used for pupil dilation are routinely used in clinical practice. Side effects are very uncommon, other than the expected blurred vision and light sensitivity.

Future

When continuing to evaluate the PIMD-2π method in the future, a larger sample size should be used.

Similar investigations as the current study could be performed with different age groups. It has been seen histologically that a natural loss of nerve fibers in the retina occurs with age [14]. The same was observed with the BMO-MRW parameter [24], and would be of value to confirm with the PIMD-2π method as well. Before OCT examination the subjects refractivre error should be measured - in part to ensure that it falls within the inclusion criteria, and in part to be able to make comparisons between groups with different errors. Thereby the question of the effect of ONH tilt on PIMD measurements could be answered.

Further correlation between ocular dominance and nerve fiber layer thickness in the ONH requires testing of dominance with more than one test. Subjects with eyes of uncertain dominance could then be excluded.

Regarding the diagnostic significance of PIMD, it would not be meaningful to compare a patient's PIMD-values with a reference database of "normal eyes", since the variation among individuals is large. One patient's values should instead be compared to previous measurements of the same eye. PIMD-2π might mask a change in nerve fiber layer thickness if it appears in only a small segment of the ONH. However, when comparing PIMD in each of the 500 angles with previous measurements of the same patient, the change may be visible. Because of the clear pattern, rotational positions of the eye etc. that can differ between occasions won't matter – the two curves can be matched according to the pattern. According to the analysis of variance, ten volumes of the ONH should be averaged per occasion to be able to detect a ten per cent loss of in the average nerve fiber layer. One might argue that ten is a large number of volumes for one person to have to sit still and focus. Though, an OCT examination with ten volumes would probably not take longer time than a visual field perimetry examination.

The time consuming part of the PIMD-2π method instead lies within the PIMD estimation process. With one volume taking around seven minutes to manually delineate, complete automation of the method would have to be achieved before considering using it in clinical practice.

Conclusions

There is a clear pattern in angular PIMD in the frontal plane. The pattern is of similar appearance both among eyes within an individual, and among individuals. The nerve fiber layer is thicker in the superior and, in particular, inferior pole of the ONH. PIMD-2π does not seem to depend on gender or ocular dominance.

In order to detect a 10 % loss of the nerve fiber layer in follow-up of glaucoma, 10 volumes of the ONH per examination occasion would yield sufficient precision.

Acknowledgements

References

1. Tham, Y.-C. *et al.* Global Prevalence of Glaucoma and Projections of Glaucoma Burden through 2040. *Ophthalmology* **121,** 2081–2090 (2014).
2. Quigley, H. A. The number of people with glaucoma worldwide in 2010 and 2020. *Br. J. Ophthalmol.* **90,** 262–267 (2006).

3. Kolko, M., Horwitz, A., Thygesen, J., Jeppesen, J. & Torp-Pedersen, C. The Prevalence and Incidence of Glaucoma in Denmark in a Fifteen Year Period: A Nationwide Study. *PLOS ONE* **10,** e0132048 (2015).

4. Weinreb, R. N., Aung, T. & Medeiros, F. A. The Pathophysiology and Treatment of Glaucoma: A Review. *JAMA* **311,** 1901 (2014).

5. Weinreb, R. N. & Khaw, P. T. Primary open-angle glaucoma. *The Lancet* **363,** 1711–1720 (2004).

6. Sommer, A. *et al.* Clinically detectable nerve fiber atrophy precedes the onset of glaucomatous field loss. *Arch. Ophthalmol.* **109,** 77–83 (1991).

7. Chauhan, B. C., Nicolela, M. T. & Artes, P. H. Incidence and Rates of Visual Field Progression after Longitudinally Measured Optic Disc Change in Glaucoma. *Ophthalmology* **116,** 2110–2118 (2009).

8. Medeiros, F. A. *et al.* Prediction of functional loss in glaucoma from progressive optic disc damage. *Arch. Ophthalmol. Chic. Ill 1960* **127,** 1250–1256 (2009).

9. Jampel, H. D. *et al.* Agreement Among Glaucoma Specialists in Assessing Progressive Disc Changes From Photographs in Open-Angle Glaucoma Patients. *Am. J. Ophthalmol.* **147,** 39–44.e1 (2009).

10. Jaffe, G. J. & Caprioli, J. Optical coherence tomography to detect and manage retinal disease and glaucoma. *Am. J. Ophthalmol.* **137,** 156–169 (2004).

11. Riordan-Eva, P. in *Vaughan & Asbury's General Ophthalmology* (eds. Riordan-Eva, P. & Cunningham, E. T.) (The McGraw-Hill Companies, 2011).

12. Levin, L. A. & Kaufman, P. L. *Adler's physiology of the eye: clinical application.* (Saunders/Elsevier, 2011).

13. Ramrattan, R. S., Wolfs, R. C., Jonas, J. B., Hofman, A. & de Jong, P. T. V. Determinants of optic disc characteristics in a general population – The Rotterdam study. *Ophthalmology* **106,** 1588–1596 (1999).

14. Jonas, J. B., Schmidt, A. M., Müller-Bergh, J. A., Schlötzer-Schrehardt, U. M. & Naumann, G. O. Human optic nerve fiber count and optic disc size. *Invest. Ophthalmol. Vis. Sci.* **33,** 2012–2018 (1992).

15. Dichtl, A., Jonas, J. B. & Naumann, G. O. Retinal nerve fiber layer thickness in human eyes. *Graefes Arch. Clin. Exp. Ophthalmol. Albrecht Von Graefes Arch. Klin. Exp. Ophthalmol.* **237,** 474–479 (1999).

16. Tariq, Y. M., Li, H., Burlutsky, G. & Mitchell, P. Retinal nerve fiber layer and optic disc measurements by spectral domain OCT: normative values and associations in young adults. *Eye* **26,** 1563–1570 (2012).

17. Huang, D. *et al.* Optical Coherence Tomography. *Science* **254,** 1178–1181 (1991).

18. Wojtkowski, M. *et al.* Three-dimensional Retinal Imaging with High-Speed Ultrahigh-Resolution Optical Coherence Tomography. *Ophthalmology* **112,** 1734–1746 (2005).

19. Choma, M. A., Hsu, K. & Izatt, J. A. Swept source optical coherence tomography using an all-fiber 1300-nm ring laser source. *J. Biomed. Opt.* **10,** 044009 (2005).

20. Považay, B. *et al.* Minimum distance mapping using three-dimensional optical coherence tomography for glaucoma diagnosis. *J. Biomed. Opt.* **12,** 041204-041204-8 (2007).

21. Chen, T. C. Spectral Domain Optical Coherence Tomography in Glaucoma: Qualitative and Quantitative Analysis of the Optic Nerve Head and Retinal Nerve Fiber Layer (An AOS Thesis). *Trans. Am. Ophthalmol. Soc.* **107,** 254–281 (2009).

22. Tsikata, E. *et al.* Comprehensive Three-Dimensional Analysis of the Neuroretinal Rim in Glaucoma Using High-Density Spectral-Domain Optical Coherence Tomography Volume Scans. *Invest. Ophthalmol. Vis. Sci.* **57,** 5498 (2016).

23. Reis, A. S. C. *et al.* Influence of Clinically Invisible, but Optical Coherence Tomography Detected, Optic Disc Margin Anatomy on Neuroretinal Rim Evaluation. *Invest. Ophthalmol. Vis. Sci.* **53,** 1852–1860 (2012).

24. Chauhan, B. C. *et al.* Bruch's Membrane Opening Minimum Rim Width and Retinal Nerve Fiber Layer Thickness in a Normal White Population. *Ophthalmology* **122,** 1786–1794 (2015).

25. Chauhan, B. C. *et al.* Enhanced Detection of Open-angle Glaucoma with an Anatomically Accurate Optical Coherence Tomography–Derived Neuroretinal Rim Parameter. *Ophthalmology* **120,** 535–543 (2013).

26. Malmberg, F., Sandberg-Melin, C. & Söderberg, P. G. Estimating a structural bottle neck for eye-brain transfer of visual information from 3D-volumes of the optic nerve head from a commercial OCT device. in **9693,** 96930N–96930N–5 (2016).

27. Sandberg Melin, C., Malmberg, F. & Söderberg, P. G. Pigment epithelium central limit-Inner limit of the retina Minimal Distance, PIMD-2π, an OCT variable for measuring glaucoma.

28. Söderberg, P. G., Malmberg, F. & Sandberg-Melin, C. Further analysis of clinical feasibility of OCT-based glaucoma diagnosis with Pigment epithelium central limit- Inner limit of the retina Minimal Distance (PIMD). in **10045,** 100450R–100450R–9 (2017).

29. Belghith, A. *et al.* Does the Location of Bruch's Membrane Opening Change Over Time? Longitudinal Analysis Using San Diego Automated Layer Segmentation Algorithm (SALSA). *Invest. Ophthalmol. Vis. Sci.* **57,** 675–682 (2016).

30. Almobarak, F. A. *et al.* Automated Segmentation of Optic Nerve Head Structures With Optical Coherence Tomography. *Invest. Ophthalmol. Vis. Sci.* **55,** 1161–1168 (2014).

31. Reiss, M. & Reiss, G. Ocular Dominance: Some Family Data. *Laterality Asymmetries Body Brain Cogn.* **2,** 7–16 (1997).

32. Ehrenstein, W. H., Arnold-Schulz-Gahmen, B. E. & Jaschinski, W. Eye preference within the context of binocular functions. *Graefes Arch. Clin. Exp. Ophthalmol.* **243,** 926–932 (2005).

33. Seijas, O. *et al.* Ocular Dominance Diagnosis and Its Influence in Monovision. *Am. J. Ophthalmol.* **144,** 209–216.e1 (2007).

34. Samarawickrama, C. *et al.* Macular thickness, retinal thickness, and optic disk parameters in dominant compared with nondominant eyes. *J. AAPOS Off. Publ. Am. Assoc. Pediatr. Ophthalmol. Strabismus* **13,** 142–147 (2009).

35. Choi, J. A., Kim, J.-S., Park, H.-Y. L., Park, H. & Park, C. K. Retinal nerve fiber layer thickness profiles associated with ocular laterality and dominance. *Neurosci. Lett.* **558,** 197–202 (2014).

36. Jee, D., Hong, S. W., Jung, Y. H. & Ahn, M. D. Interocular Retinal Nerve Fiber Layer Thickness Symmetry Value in Normal Young Adults: *J. Glaucoma* **23,** e125–e131 (2014).

37. Hwang, Y. H., Song, M., Kim, Y. Y., Yeom, D. J. & Lee, J. H. Interocular symmetry of retinal nerve fibre layer thickness in healthy eyes: a spectral-domain optical coherence tomographic study: Interocular symmetry of retinal nerve fibre layer thickness. *Clin. Exp. Optom.* **97,** 550–554 (2014).

38. Miles, W. R. Ocular dominance demonstrated by unconscious sighting. *J. Exp. Psychol.* **12,** 113 (1929).

39. Knight, O. J. *et al.* Effect of Race, Age, and Axial Length on Optic Nerve Head Parameters and Retinal Nerve Fiber Layer Thickness Measured by Cirrus HD-OCT. *Arch. Ophthalmol.* **130,** 312–318 (2012).

40. Hwang, Y. H., Yoo, C. & Kim, Y. Y. Myopic Optic Disc Tilt and the Characteristics of Peripapillary Retinal Nerve Fiber Layer Thickness Measured by Spectral-domain Optical Coherence Tomography: *J. Glaucoma* **21,** 260–265 (2012).

41. Asai, T. *et al.* Analysis of Peripapillary Geometric Characters in High Myopia Using Swept-Source Optical Coherence TomographyPeripapillary Geometric Characters In High Myopia. *Invest. Ophthalmol. Vis. Sci.* **57,** 137–144 (2016).

42. You, Q. S., Xu, L. & Jonas, J. B. Tilted optic discs: the Beijing eye study. *Eye* **22,** 728–729 (2008).